temperature leads to exciplex formation and the green emission from the $[CuCu]^{2+}$ excimer and the orange emission from the $[CuAg]^{2+}$ exciplex. No emission from a $[AgAg]^{2+}$ excimer is found. Cooling of a crystal during irradiation of a spot causes trapping of the dimers in that spot. The luminescence spectrum and intensity from the trapped dimers in the written spot are different from those of the unirradiated portions of the crystal. These changes are an example of optical memory. The emission, absorption, and excitation spectra of the crystals are dependent on the temperature and the Ag^+ ion concentration.

Acknowledgment. The research was supported by the U.S. Office of Naval Research (J.D.B. and B.D.) and by the NSF CHE 88-06775 (K.-S.K.S. and J.I.Z.). We thank Leslie Momoda for her help in preparing the crystals and Gary Hollingsworth for preliminary measurements.

Registry No. Ag, 14701-21-4; Cu, 17493-86-6; alumina, 1344-28-1.

An Integral Equation Theory Study of the Solvent-Induced Reaction Barrier in the Nucleophilic Addition of Hydroxide to Formaldehyde

Hsiang-Ai Yu and Martin Karplus*

Contribution from the Department of Chemistry, Harvard University, Cambridge, Massachusetts 02138. *Received June 28, 1989*

Abstract: The solvent-induced reaction barrier in water for the nucleophilic addition of hydroxide anion to formaldehyde is studied by integral equation theory and compared with Monte Carlo [Madura, J. D.; Jorgensen, W. L. *J. Am. Chem. Soc.* **1986**, *108*, 2517] and molecular dynamics results. The free energy profile correlates well with the charge transfer during the reaction. The position of the transition state is shifted from R_{C-O2} = 2.39 Å in the gas phase to 2.0 Å in water, in agreement with the Monte Carlo simulation. The activation free energy of 21 kcal/mol is in approximate agreement with experimental data on esters and amides (15–19 kcal/mol for alkaline hydrolysis of esters and 22–24 kcal/mol for amides) but is significantly larger than an experimental estimate (9 kcal/mol) for formaldehyde from a rate constant measurement at a single temperature. Since the Monte Carlo simulation also gave values of 24–28 kcal/mol, the difference is surprising and suggests that a more detailed experimental study of the reaction rate as a function of temperature would be of interest. The tetrahedral complex is 13 kcal/mol lower in free energy than the transition state, in agreement with 10–14 kcal/mol from the simulation. Detailed analyses of the enthalpic and entropic terms are made and the potential of mean force is decomposed into contributions from the individual sites. The reaction profile is dominated by an enthalpy barrier of 26–28 kcal/mol for addition and 12 kcal/mol for dissociation. The success of the present thermodynamic calculation demonstrates the utility of the computationally less demanding analytic integral equation theory for exploration of alternative reaction mechanisms. However, the fact that radial distribution functions show only qualitative agreement with the simulation results suggests that there may be a cancellation of errors and that care must be used in interpreting the results.

1. Introduction

Organic reactions involving the carbonyl group, –CO–, are widespread in chemistry and biology. Amide or ester hydrolysis and synthesis, for example, play essential roles in the formation and destruction of the peptide unit, –NH–CO–, that links amino acids together to form proteins. The carbonyl carbon is the site of nucleophilic attack and the hydrolysis may be catalyzed by acid or base.[1] A case of biological interest is provided by the family of serine proteases.[2] For the forward reaction, in which the peptide substrate is hydrolyzed, it is generally accepted that a serine side-chain hydroxyl attacks the carbonyl carbon to form an acyl intermediate.[2] In the deacylation stage, a hydroxide anion or otherwise activated species derived from water is the nucleophile that displaces the acyl polypeptide by attacking the same carbonyl carbon. Schematically the deacylation can be represented as

$$OH^- + R_1R_2C{=}O \rightarrow [R_1{-}\overset{\overset{O}{|}}{\underset{\underset{OH}{|}}{C}}{-}R_2]^- \rightarrow R_1H + R_2COO^- \quad (1)$$

where R_1– is the enzyme, and R_2CO– is the leaving acyl group. A pair of peptide backbone NHs contribute to the catalysis by coordinating the carbonyl oxygen in the same proteases. An imidazole side chain is involved in activating the water.[3]

We report here an extended reference interaction site model (RISM) integral equation study[4] of the first step in scheme 1 for a simplified model reaction where both R groups are hydrogens; i.e., the attack of OH^- on the carbonyl of formaldehyde. We study this system because of its role as a well-studied prototype of nucleophilic addition to the carbonyl group.[5] Also, there exist a large number of gas-phase theoretical studies,[6-9] as well as the Monte Carlo (MC) solvation study of Madura and Jorgensen.[10] This work provides an opportunity to compare in detail the performance of the integral equation theory with an MC simulation of a reaction. Of particular interest is the result that while in the gas phase the approach of OH^- to H_2CO is dominated by an attractive ion–dipole interaction; the variation in solvation free energy along the reaction coordinate gives rise to a barrier. In nature, formaldehyde interacts with water to form a diol;[11] in the present model study, this reaction is not considered.

(1) Carey, F. A.; Sundberg, R. J. *Advanced Organic Chemistry, Part A*; Plenum Press: New York, 1977.
(2) Fersht, A. *Enzyme Structure and Mechanism. Freeman*; New York, 1985.
(3) Kraut, J. *Annu. Rev. Biochem.* **1977**, *46*, 331.
(4) Hirata, F.; Rossky, P. J. *Chem. Phys. Lett.* **1981**, *83*, 329.
(5) Riveros, J. M.; Jose, S. M.; Takashima, K. *Adv. Phys. Org. Chem.* **1985**, *21*, 197.
(6) Alagona, G.; Ghio, C.; Kollman, P. A. *J. Am. Chem. Soc.* **1985**, *107*, 2229.
(7) Burgi, H. B.; Lehn, J. M.; Wipff, G. *J. Am. Chem. Soc.* **1974**, *96*, 1956.
(8) Williams, I. H. *J. Am. Chem. Soc.* **1987**, *109*, 6299.
(9) Howard, A. E.; Kollman, P. A. *J. Am. Chem. Soc.* **1988**, *110*, 7195.
(10) Madura, J. D.; Jorgensen, W. L. *J. Am. Chem. Soc.* **1986**, *108*, 2517. In accord with this reference, we distinguish the hydrogens and oxygens of formaldehyde with label 1 and those of the hydroxide with label 2 when there is a possibility of confusion; those of the aqueous solvent are labeled with subscript w.
(11) Zavitsas, A. A.; Coffiner, M.; Wiseman, T.; Zavitsas, L. R. *J. Phys. Chem.* **1970**, *74*, 2746.

0002-7863/90/1512-5706$02.50/0

The integral equation theory used in this paper is the reference interaction site model (RISM) equation of Chandler and Andersen[12] and its extension by Rossky and co-workers to polar systems.[4,13-15] Applications to studies of liquid structures,[16,17] hydrophobic effect,[18-20] and ionic solvation[13,14] have demonstrated its usefulness. The method has also been employed to study chemical reactions in solution (e.g., the S_N2 reaction of Cl^- and CH_3Cl;[15] ion-pair formation/dissociation of *tert*-butyl$^+$:Cl^-;[21] the $Fe^{2+} \rightleftharpoons Fe^{3+}$ ionic equilibrium[22]) and isomerization in condensed phases (e.g., cyclohexane in CS_2;[23] butane in water[24]). The systems investigated range from nonpolar solutes in nonpolar solvents to multiply charged ions in water. The accuracy of the integral equation results, when compared to simulations or experiment, is not uniform. Excellent results were obtained for the S_N2 reaction of Cl^- and CH_3Cl where the barrier in solution calculated from the HNC-RISM (the RISM integral equation coupled with the site-site hypernetted chain, HNC, closure)[4] is 31 kcal/mol,[15] in good agreement with values of 26–27 kcal/mol from experiment and other theoretical studies.[25,26] The worst case is one with much stronger interactions, in which divalent and trivalent cations were studied. The HNC–RISM predicted an activation free energy of 44 kcal/mol[22] for $Fe^{2+} \rightleftharpoons Fe^{3+}$, much higher than the value of 15–20 kcal/mol from experiment[27] and a simulation.[28] In both reactions, the position of the barrier can be predicted a priori from symmetry considerations. For the *tert*-butyl$^+$:Cl^- ion pair in water, the HNC–RISM result gave a dissociation barrier of 0.46 kcal/mol at 3.6-Å separation between Cl^- and the central carbon of the *tert*-butyl$^+$ group; a barrier of 2.1 kcal/mol at 4.1 Å was obtained from a Monte Carlo simulation.[21] The contact ion pair at 2.9 Å in the simulation is 2.5 kcal/mol higher in energy than in the HNC–RISM result. The integral equation thus predicted a different position (off by 0.5 Å) for the transition state and a smoother potential of mean force. This reactions involves two charged species interacting to give an overall neutral product without charge transfer between them. Thus, more studies are needed to validate the HNC–RISM method for cases where thermodynamic and structural results can be compared with experimental and/or simulation data.

In addition to determining the potential of mean force (PMF) along the reaction coordinate and comparing the results with those of a Monte Carlo simulation we use density and temperature derivatives in the RISM formalism[24,29,30] to evaluate the enthalpy (energy) and entropy contributions to the PMF. This is very difficult to do by MC or molecular dynamics simulation because of convergence problems. It has been shown that by use of the experimental dielectric constant and the isobaric thermal expansion coefficient for water the solvation enthalpy for monovalent ions Cl^-, Br^-, Na^+, and K^+ can be calculated with the RISM integral equation theory and that the results are in satisfactory (~10%) agreement with experimental data.[30] The underestimation of the solvent dielectric constant and its effect on the solute PMF are corrected by modifying the closure for the solvent correlation functions to ensure consistency in their long-range behavior.[31-33] This approach, in contrast to an earlier method,[15,33] can be applied to chemical reactions involving charge transfer where the solutes have nonzero charges at small separation but are neutral at infinite separation.

In section 2, we summarize the methods of calculation. The results and discussion are given in section 3. The conclusions are summarized in section 4.

2. Methods

2.1. Theory. In this section, we give a brief account of the integral equation theory; the references cited should be consulted for details.[4,16,29,30] For the case of a solute (u) dissolved in a solvent (v) at infinite dilution [$\rho_u \rightarrow 0$, denoted by superscript (o)], the vv and uv parts of the RISM integral equation[4,12,13,16] cast in matrix (denoted by boldface letters) form in Fourier k-space (denoted by a caret) are

$$\hat{\mathbf{h}}^{(o)}_{\alpha v} = \hat{\mathbf{Q}}^{(o)}_{\alpha v} + [\hat{\mathbf{w}}_\alpha \hat{\mathbf{c}}^{*(o)}_{\alpha v} + \hat{\mathbf{Q}}^{(o)}_{\alpha v}\rho_v \hat{\mathbf{c}}^{*(o)}_{vv}][\hat{\mathbf{w}}_v + \rho_v \hat{\mathbf{h}}^{(o)}_{vv}] \quad (2)$$

$$\hat{\mathbf{Q}}^{(o)}_{\alpha v} = \hat{\mathbf{w}}_\alpha \hat{\phi}'_{\alpha v}[\hat{\mathbf{w}}_v + \rho_v \hat{\mathbf{Q}}^{(o)}_{vv}] \quad (3)$$

where $\{\alpha\} = \{u, v\}$. In eqs. 2 and 3, $\hat{\mathbf{h}}$ is the matrix of intermolecular total correlation functions; $\hat{\mathbf{Q}}$ is the chain sum of $\hat{\phi}$[34] where $\hat{\phi}'_{\alpha v} = (\delta^u_\alpha + A\delta^v_\alpha)\hat{\phi}_{\alpha v}$ with $\hat{\phi}_{\alpha\gamma}(k) = 4\pi\beta z_\alpha z_\gamma/k^2$; $\beta = 1/k_B T$, k_B is the Boltzmann constant, T is the temperature, and z_α is the charge on site α. The symbol A corresponds to a numerical factor introduced into the site–site HNC closure

$$h^{(o)}_{\alpha v}(r) = \exp\{-\beta U^*_{\alpha v}(r) + (\delta^u_\alpha + A\delta^v_\alpha)\phi_{\alpha v}(r) + h^{(o)}_{\alpha v}(r) - c^{(o)}_{\alpha v}(r)\} - 1 \quad (4)$$

to ensure consistency between the long-ranged behavior of calculated *solvent* (hence the associated Kronecker δ^v_α) correlation functions and a given value of the *solvent* dielectric constant, ϵ_0. A is given by[31-33]

$$A = \frac{1 + \epsilon_0(3y - 1)}{3y(\epsilon_0 - 1)}$$

with

$$y = \frac{4\pi\beta\rho_v\langle d_v^2\rangle}{9} \quad (5)$$

where $\langle d_v^2\rangle$ is the average squared dipole moment of the solvent molecule. The symbol $\hat{\mathbf{w}}$ is the matrix of intramolecular correlation functions; $\hat{\mathbf{c}}^* = \hat{\mathbf{c}} - \hat{\phi}'$ in which $\hat{\mathbf{c}}$ is the direct correlation function matrix; ρ_v is the matrix of solvent density. For rigid molecules, $\hat{w}_{\alpha\gamma}(k) = (\sin kL_{\alpha\gamma})/kL_{\alpha\gamma}$ with $L_{\alpha\gamma}$ the distance between sites α and γ. U^* is a short-ranged potential that usually, but not necessarily, takes the Lennard-Jones 6–12 form. Comparing eq 4 with the common form of the HNC closure, $h(r) = \exp\{-\beta U(r) + h(r) - c(r)\} - 1$ where $U = U^* - \phi/\beta$ is the total intermolecular potential, we can identify an effective potential $U^{eff}_{vv} = U^*_{vv} - A\phi_{vv}/\beta$ for the solvent.

By solving eqs 2–4 one can calculate the excess solvation free energy, $\Delta\mu^{(o)}_{u,sol}$, of introducing a solute into the solvent at infinite dilution from the expression[24,35]

$$\Delta\mu^{(o)}_{u,sol} = \frac{\rho_v}{\beta}\sum_{\alpha=1}^{n_u}\sum_{\gamma=1}^{n_v}\int d\vec{r}\left\{\frac{1}{2}[h^{(o)}_{\alpha\gamma}(r)]^2 - c^{(o)}_{\alpha\gamma}(r) - \frac{1}{2}h^{(o)}_{\alpha\gamma}(r)c^{(o)}_{\alpha\gamma}(r)\right\} \quad (6)$$

To decompose $\Delta\mu^{(o)}_{u,sol}$ into enthalpy (or energy) and entropy, the temperature and density derivatives of eqs 2–4 can be used. For the first-order isochoric temperature derivatives, we have[30]

$$\delta_T\hat{h}^{(o)}_{\alpha\gamma} = \hat{\mathbf{w}}_\alpha[\delta_T\hat{\mathbf{c}}^{(o)}_{\alpha\gamma}\hat{\mathbf{w}}_\gamma + \delta_T\hat{\mathbf{c}}^{(o)}_{\alpha v}\rho_v\hat{\mathbf{h}}^{(o)}_{v\gamma}] + \hat{\mathbf{h}}^{(o)}_{\alpha v}\rho_v[\delta_T\hat{\mathbf{c}}^{(o)}_{v\gamma}\hat{\mathbf{w}}_\gamma + \delta_T\hat{\mathbf{c}}^{(o)}_{vv}\rho_v\hat{\mathbf{h}}^{(o)}_{v\gamma}] \quad (7)$$

(12) Chandler, D.; Andersen, H. C. *J. Chem. Phys.* **1972**, *57*, 1930.
(13) Hirata, F.; Rossky, P. J.; Pettitt, B. M. *J. Chem. Phys.* **1983**, *78*, 4133.
(14) Pettitt, B. M.; Rossky, P. J. *J. Chem. Phys.* **1982**, *77*, 1451.
(15) Chiles, R. A.; Rossky, P. J. *J. Am. Chem. Soc.* **1984**, *106*, 6867.
(16) Chandler, D. In *The Liquid State of Matter: Fluids, Simple and Complex*; Montroll, E. W., Lebowitz, J. L., Ed.; North-Holland: New York, 1982; Vol. 8, 275.
(17) Hirata, F.; Pettitt, B. M.; Rossky, P. J. *J. Chem. Phys.* **1982**, *77*, 509.
(18) Pratt, L. R.; Chandler, D. *J. Chem. Phys.* **1977**, *67*, 3683.
(19) Pratt, L. R.; Chandler, D. *J. Chem. Phys.* **1980**, *73*, 3434.
(20) Ichiye, T.; Chandler, D. *J. Phys. Chem.* **1988**, *92*, 5257.
(21) Jorgensen, W. L.; Buckner, J. K.; Huston, S. E.; Rossky, P. J. *J. Am. Chem. Soc.* **1987**, *109*, 1891.
(22) Kuharski, R. A.; Chandler, D. *J. Phys. Chem.* **1987**, *91*, 2978.
(23) Singer, S. J.; Kuharski, R. A.; Chandler, D. *J. Phys. Chem.* **1986**, *90*, 6015.
(24) Zichi, D. A.; Rossky, P. J. *J. Chem. Phys.* **1986**, *84*, 1712.
(25) Chandrasekhar, J.; Smith, S. F.; Jorgensen, W. L. *J. Am. Chem. Soc.* **1985**, *107*, 154.
(26) Bash, P.; Field, M.; Karplus, M. *J. Am. Chem. Soc.* **1987**, *109*, 8092.
(27) Silverman, J.; Dodson, R. W. *J. Phys. Chem.* **1952**, *56*, 846.
(28) Kuharski, R. A.; Bader, J. S.; Chandler, D.; Sprik, M.; Klein, M. L.; Impey, R. W. *J. Chem. Phys.* **1989**, *89*, 3248.
(29) Yu, H. A.; Karplus, M. *J. Chem. Phys.* **1988**, *89*, 2366.
(30) Yu, H. A.; Roux, B.; Karplus, M. *J. Chem. Phys.* **1990**, *92*, 5020.
(31) Cummings, P. J.; Stell, G. *Mol. Phys.* **1981**, *44*, 529.
(32) Cummings, P. J.; Stell, G. *Mol. Phys.* **1982**, *46*, 383.
(33) Rossky, P. J.; Pettitt, B. M.; Stell, G. *Mol. Phys.* **1983**, *50*, 1263.
(34) Rossky, P. J.; Dale, W. D. T. *J. Chem. Phys.* **1980**, *73*, 2457.
(35) Singer, S. J.; Chandler, D. *Mol. Phys.* **1985**, *55*, 621.

Table I. Summary of Molecular Dynamics Simulations of Solutes in TIP3P Water

system	⟨T⟩,[a] K	TIP3P no.	time, ps equilbrtn	time, ps prodtn
H_2CO	299	305	12	25
OH^-	299	306	15	35
transition state	303	302	10	25
product	303	302	10	25

[a] Average temperature. The OH^- simulation used velocity scaling to keep the temperature near 298.15 K.

where $\{\alpha, \gamma\} = \{u, v\}$ and $\delta_T\hat{\mathbf{c}}^{(o)} = \delta_T\hat{\mathbf{c}}^{*(o)} - \hat{\phi}''$ with $\hat{\phi}''_{\alpha v} = [(\delta_T A - A/T)\delta^v_\alpha - \delta^u_\alpha/T]\hat{\phi}_{\alpha v}$. The temperature derivative of the HNC closure is given by

$$\delta_T h^{(o)}_{\alpha\gamma}(r) = \left[\frac{\beta}{T}U^*_{\alpha\gamma}(r) + \delta_T h^{(o)}_{\alpha\gamma}(r) - \delta_T c^{*(o)}_{\alpha\gamma}(r)\right][h^{(o)}_{\alpha\gamma}(r) + 1] \tag{8}$$

For the first-order isothermal density derivatives, we have[29,30]

$$\delta\rho_\eta\hat{\mathbf{h}}^{(o)}_{\alpha\gamma} = \hat{\mathbf{w}}_\alpha\delta\rho_\eta\hat{\mathbf{c}}^{(o)}_{\alpha\gamma}\hat{\mathbf{w}}_\gamma + [\hat{\mathbf{w}}_\alpha\delta\rho_\eta\hat{\mathbf{c}}^{(o)}_{\alpha v} + \hat{\mathbf{h}}^{(o)}_{\alpha v}\rho_v\delta\rho_\eta\hat{\mathbf{c}}^{(o)}_{vv}]\rho_v\hat{\mathbf{h}}^{(o)}_{v\gamma} + \hat{\mathbf{h}}^{(o)}_{\alpha\eta}\hat{\mathbf{w}}^{-1}_\eta\hat{\mathbf{h}}^{(o)}_{\eta\gamma} \tag{9}$$

where $\{\alpha, \gamma, \eta\} = \{u, v\}$ and $\delta_{\rho_\eta}\hat{\mathbf{c}}^{(o)} = \delta_{\rho_\eta}\hat{\mathbf{c}}^{*(o)} + \hat{\phi}^\eta$ with $\hat{\phi}^\eta_{\alpha\gamma} = (\delta_{\rho_\eta}A)\hat{\phi}_{\alpha\gamma}$. The corresponding density derivative of the HNC closure is

$$\delta\rho_\eta h^{(o)}_{\alpha\gamma}(r) = [\delta\rho_\eta h^{(o)}_{\alpha\gamma}(r) - \delta\rho_\eta c^{*(o)}_{\alpha\gamma}(r)][h^{(o)}_{\alpha\gamma}(r) + 1] \tag{10}$$

The solvation enthalpy is given by[30]

$$\Delta h^{(o)}_{u,sol} = \Delta\epsilon^{(o)}_{u,sol} + T\alpha_{v,P}\left\{\Delta\mu^{(o)}_{u,sol} + \frac{\rho_v^2}{2\beta}\sum_{\alpha=1}^{n_u}\sum_{\gamma=1}^{n_v}\int d\vec{r}[h^{(o)}_{\alpha\gamma}(r)\delta\rho_v c^{(o)}_{\alpha\gamma}(r) - c^{(o)}_{\alpha\gamma}(r)\delta\rho_v h^{(o)}_{\alpha\gamma}(r)]\right\} \tag{11}$$

where $\alpha_{v,P}$ is the isobaric thermal expansion coefficient of the pure solvent. Here $\Delta\epsilon^{(o)}_{u,sol}$ is the solvation energy that can be calculated from either a temperature derivative of the solvation free energy[30]

$$\Delta\epsilon^{(o),T}_{u,sol} = \rho_v\sum_{\alpha=1}^{n_u}\sum_{\gamma=1}^{n_v}\int d\vec{r}U_{\alpha\gamma}(r)[1 + h^{(o)}_{\alpha\gamma}(r)] + \frac{T\rho_v}{2\beta}\sum_{\alpha=1}^{n_u}\sum_{\gamma=1}^{n_v}\int d\vec{r}[c^{(o)}_{\alpha\gamma}(r)\delta_T h^{(o)}_{\alpha\gamma}(r) - h^{(o)}_{\alpha\gamma}(r)\delta_T c^{(o)}_{\alpha\gamma}(r)] \tag{12}$$

or a density derivative[29]

$$\Delta\epsilon^{(o),\rho}_{u,sol} = \rho_v\sum_{\alpha=1}^{n_u}\sum_{\gamma=1}^{n_v}\int d\vec{r}U_{\alpha\gamma}(r)[1 + h^{(o)}_{\alpha\gamma}(r)] + \frac{\rho_v^2}{2}\sum_{\eta=1}^{n_u}\sum_{\gamma=1}^{n_v}\int d\vec{r}U_{\gamma\eta}(r)\delta\rho_u h^{(o)}_{\gamma\eta}(r) \tag{13}$$

where the superscripts T and ρ have been used to distinguish whether the solvation energy was calculated from a temperature or a density derivative, respectively. The difference between eqs. 12 and 13 lie in the second term that originates from solvent reorganization.[29,30] In general, the two expressions give different numerical results that provide some indication of the errors inherent in the approximate integral equation. The solvation entropy is obtained from the difference between eqs. 6 and 11, using either 12 or 13 for the energy.

In addition to the HNC–RISM calculations, a microcanonical molecular dynamics simulation with periodic boundary condition was used to study the reaction. Four sets of simulations in a cubic box of length 21 Å are summarized in Table I. The number of water molecules range from 302 to 306 giving densities near 0.99 g/cm^3. The equation of motion was integrated with a time step of 1 fs. The nonbond list was updated every 20 fs and the coordinates were saved every 5 fs for analysis. A third-order switching function smoothly turns off the nonbond interaction from 7.5 to 8.5 Å based on groups.[36] The SHAKE[37] algorithm was used to remove all intramolecular degrees of freedom in the solutes, as well as the aqueous solvent. Since SHAKE constrains distances, there are numerical problems that prevent its application to planar molecules of more than three atoms. Two dummy (i.e., *noninteracting*) atoms were therefore introduced in the planar formaldehyde simulation and all distances between the dummy atoms and the formaldehyde atoms were kept fixed. The dummy atoms were assigned the mass of hydrogen and were positioned at 0.5 Å from the carbonyl carbon on both sides perpendicular to the plane of H_2CO to preserve the C_s symmetry. Although the total mass of the formaldehyde is increased by 7%, this does not change the equilibrium properties that depend only on the configurational space. However, in practice, small differences in the convergence of finite simulations may result. In the hydroxide anion simulation, the strong electrostatic interaction between the hydroxide and water induces large fluctuations in the total potential energy. It was found necessary to apply velocity scaling every 0.2 ps such that the average temperature was kept near 298.15 K; scaling was not required for the other simulations. The molecular mechanics program CHARMM[36] was used for the simulation study.

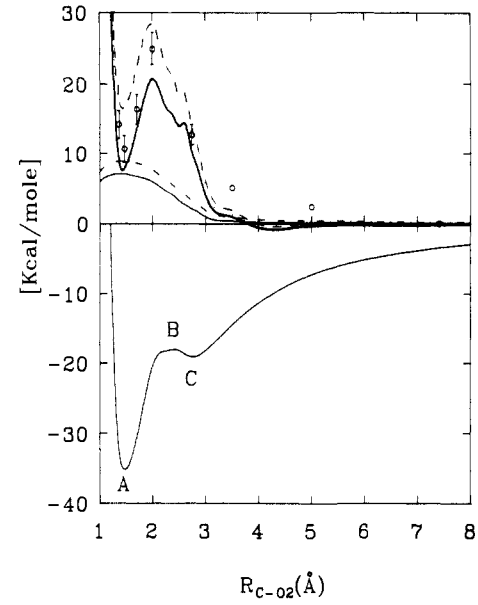

Figure 1. Energy profile in the gas phase and in water for the OH^- + H_2CO reaction. Lower panel: $U(r)$, 6-31+G* gas phase profile from ref 10. Upper panel: (—) $\Delta\mu^{(o)}_{u,sol}(r) + U(r)$; (···) $\Delta h^{(o),T}_{u,sol}(r) + U(r)$; (- - -) $\Delta h^{(o),\rho}_{u,sol}(r) + U(r)$; (—) $T\Delta s^{(o),T}_{u,sol}(r)$; (-·-) $T\Delta s^{(o),\rho}_{u,sol}(r)$; for definitions, see text. The open circles with error bars are averages and estimates from the MC simulation results.[10]

2.2. Models. The model reaction studied here is the nucleophilic addition of hydroxide anion to formaldehyde in water. We use the ab initio 6-31+G* gas-phase results given in ref 10 as the basis of our study. The gas-phase potential energy surface taken from Table II in ref 10 is shown in the lower panel of Figure 1. The solute geometric parameters as a function of the reaction coordinate, R_{C-O2} where O2 is the hydroxide oxygen, are given in Table III of the same reference.[10] It is characterized by a collinear approach up to ~2.74 Å (Figure 2, C) that changes into a tetrahedral approach at 2.39 Å (Figure 2, B); the formation of a tetrahedral complex is complete at 1.47 Å (Figure 2, A). The Lennard-Jones parameters and gas-phase partial charges for the reactants, the transition states (in gas and in solution phases) and the tetrahedral complex are given in Table II; they were taken from Table V of ref 10. To fit the quantum mechanical interaction energies with a single TIP4P water molecule, the σ and ϵ values,

(36) Brooks, B. R.; Bruccoleri, R. E.; Olafson, B. D.; States, D. J.; Swaminathan, S.; Karplus, M. *J. Comput. Chem.* **1983**, *4*, 187.
(37) Ryckaert, J.-P.; Ciccotti, G.; Berendsen, H. J. C. *J. Comput. Phys.* **1977**, *23*, 327.

Table II. Lennard-Jones Parameters and Partial Charges (q) for the Solute[a]

R_{C-O2}, Å	H1, q	C			O1		H2,	O2		
		σ	ϵ	q	ϵ	q	q	σ	ϵ	q
∞	0.10	3.75	0.105	0.18	0.20	−0.38	0.30	3.20	0.25	−1.30
			(0.0)					(−1.0)		
2.39[b]	0.04	3.84	0.113	0.304	0.225	−0.59	0.336	3.13	0.205	−1.13
			(−0.206)					(−0.794)		
2.00[c]	−0.01	3.86	0.1155	0.36	0.21	−0.7	0.35	3.10	0.195	−0.99
			(−0.36)					(−0.64)		
1.47	−0.06	3.905	0.117	0.416	0.20	−0.9	0.364	3.07	0.175	−0.76
			(−0.604)					(−0.396)		

[a] Units for q in atomic unit, σ in Å, and ϵ in kcal/mol. Net charges are in parentheses. The (σ, ϵ) for H1 and H2 are (1.3, 0.03) and (0.4, 0.049 58), respectively. The σ for O1 is 3.2 Å. [b] Transition state in gas phase. [c] Transition state in water.

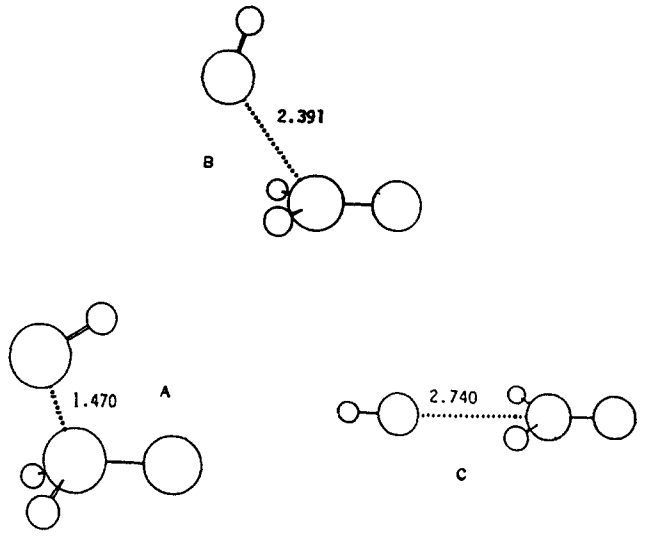

Figure 2. Structures along the gas-phase reaction path. A, tetrahedral complex; B, transition state; C, ion–dipole intermediate.

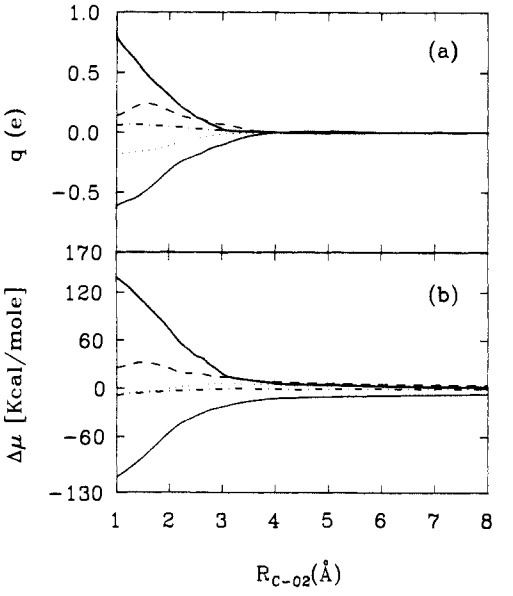

Figure 3. Charge and free energy decompositions. (—) O_2; (-·-) H2; (---) C; (···) H1; (—) O1. (a) Variation of site charges as a function of the reaction coordinate with the reactant as the reference; the reactant values are listed in Table II. (b) Site decomposition of the solvation free energy.

as well as the charges (q), were altered along the reaction path. From the reactants to the tetrahedral complex, there is a net charge transfer of −0.604 from OH^- to H_2CO, with 85% of the negative charge divided between the two oxygen sites. In Figure 3a we plot the partial charges at each site along the reaction coordinate relative to the infinitely separated reactants. The maximum in the carbonyl carbon curve (---) corresponds to a charge of 0.42 near R_{C-O2} = 1.6 Å and occurs close to the top of the barrier of the solvation free energy, $\Delta\mu^{(o)}_{u,sol}$ (see below). At R_{C-O2} = 1.0, 1.3, 1.4, 2.28, 2.5, 2.62, 2.74, 2.85, 3.0, 3.4, 4.0, 6.0, 8.0, 10.0, and 12.0 Å where additional HNC–RSIM calculations were done, the same source for parameters was used.[10] The combination rules of ref 10 were employed to facilitate comparisons; i.e., $\epsilon_{\alpha\gamma} = (\epsilon_\alpha\epsilon_\gamma)^{1/2}$ and $\sigma_{\alpha\gamma} = (\sigma_\alpha\sigma_\gamma)^{1/2}$ are used for the solute–water interaction except for the hydroxide hydrogen (H2) and water hydrogens (H_w). The combination rule $\sigma_{\alpha\gamma} = (\sigma_\alpha + \sigma_\gamma)/2$ is used when $\{\alpha\}$ = {H2, H_w} and γ is any other site. The H2 and H_w have zero Lennard-Jones parameters in ref 10. In the HNC–RISM calculation, nonzero σ values are required to remove a Coulombic singularity.[14] For the water hydrogens, values of (σ, ϵ) = (0.4 Å, 0.046 kcal/mol) were used.[38] For the hydroxide hydrogen, a range of σ_{H2} = 0.4–1.2 Å with a fixed ϵ = 0.046 kcal/mol was tested for the reactants, the transition state, and the tetrahedral complex. Within this range the hydroxide hydrogen is embedded in the van der Waals sphere of the hydroxide oxygen. The calculated solvation thermodynamics were not changed by the use of different σ_{H2} despite some changes in the distribution functions; the value σ_{H2} = 0.4 Å was adopted.

In the MC simulation,[10] the water is the rigid four-site TIP4P model.[39] In this study, we use the rigid three-site TIP3P[39] water with minor modification. Nonzero hydrogen Lennard-Jones interaction parameters were introduced to remove a Coulombic singularity.[14] The TIP3P empirical potential is characterized by an experimental water geometry (R_{OH} = 0.9572 Å, $\angle_{HOH}$ = 104.52°) and a charge of −0.834 on the oxygen site. The Lennard-Jones parameters for the oxygen site are (σ, ϵ) = (3.15 Å, 0.152 kcal/mol). For interaction between oxygen and hydrogen sites, the combination rules $\epsilon_{\alpha\gamma} = (\epsilon_\alpha\epsilon_\gamma)^{1/2}$ and $\sigma_{\alpha\gamma} = (\sigma_\alpha + \sigma_\gamma)/2$

Table III. Summary of Monohydrated Solute Geometries and Interaction Energies from the ab Initio Calculations and the Empirical Potential Functions[a]

	ab initio		empirical potential			
			TIP4P		TIP3P	
R_{C-O2}	$-\Delta E$	r	$-\Delta E$	r	$-\Delta E$	r
A	4.68	2.09	4.08	2.00	4.13	2.01
B	3.78	2.15	4.07	2.00	4.10	2.02
C	24.04	1.71	24.15	1.67	23.39	1.74
D						
2.00	13.11	1.90	12.74	1.82	13.53	1.89
1.47	18.02	1.78	17.09	1.73	16.92	1.80
E						
2.00	18.36	1.77	17.66	1.66	16.88	1.74
1.47	12.59	1.90	12.86	1.73	12.88	1.82

[a] Energies in kcal/mol, r in Å. See Figure 4 for structures A–E. The data for ab initio and TIP4P are taken from ref 10.

(38) Reiher, W. E., III Ph.D. Thesis, Harvard University, Cambridge, MA, 1985.

(39) Jorgensen, W. L.; Chandrasekhar, J.; Madura, J. D.; Impey, R. W.; Klein, M. L. *J. Chem. Phys.* **1983**, *79*, 926.

Table IV. Solvent Contribution to the Free Energy, Enthalpy, and the Energy of Solvent Reorganization ($\Delta\epsilon_{cavity}$)[a]

R_{C-O2}, Å	interaction site						
	H1	C	O1	H2		O2	total
				$\Delta\mu^{(o)}_{\mu,sol}$, kcal/mol			
∞	−0.2	9.9	−5.1	35.0		−182.0	−142.7
		(4.3)			(−147.0)		
2.39[b]	3.1	29.4	−44.4	32.7		−133.2	−109.3
		(−8.8)			(−100.5)		
2.00[c]	−0.4	35.2	−61.6	31.7		−106.3	−101.8
		(−27.2)			(−74.6)		
1.47	−4.7	43.6	−96.8	29.3		−66.5	−99.8
		(−62.6)			(−37.2)		
				$\Delta h^{(o)}_{\mu,sol}$, kcal/mol			
∞	−0.7	4.6	−7.6	35.9		−198.8	−167.3
		(−4.4)		(−162.9)	[−100 ± 5][d]	[−139.7][e]	[−147 ± 13][d] [−159.8][e]
2.39[b]	2.9	25.4	−48.5	33.6		−146.0	−129.7
		(−17.3)			(−112.4)		
2.00[c]	−0.7	31.9	−67.1	32.5		−116.2	−120.3
		(−36.6)			(−83.7)		[−79 ± 12][d] [−116.6][e]
1.47	−5.0	41.2	−105.6	29.8		−72.7	−117.3
		(−74.4)			(−42.9)		[−70 ± 11][d] [−117.5][e]
				$\Delta\epsilon_{cavity}$, kcal/mol			
∞	−0.3	2.2	6.3	−32.1		179.2	155.0
		(7.9)			(147.1)		[74 ± 13][d] [71.7][e]
2.39[b]	−2.8	−21.0	45.8	−29.1		129.1	119.2
		(19.2)			(100.0)		
2.00[c]	0.8	−27.9	62.5	−28.8		103.6	111.0
		(36.2)			(74.8)		[72 ± 12][d] [40.6][e]
1.47	4.5	−34.8	95.0	−27.2		66.3	108.2
		(69.2)			(39.1)		[84 ± 11][d] [40.5][e]

[a] $\Delta h^{(o)}_{\mu,sol}$ and $\Delta\epsilon_{cavity}$ are from eqs 11 and 12, respectively. Individual sums for H_2CO and OH^- are in parentheses or in brackets. [b] Transition state in gas phase. [c] Transition state in water. [d] From ref 10. [e] From Weiner et al.[46] for OH^- + $HCONH_2$.

are used. At 298.15 K and ρ_{H_2O} = 0.997 g/cm^3, an A = 0.959 is required to match the experimental water dielectric constant of ϵ_0 = 78.4.[40]

The difference in water models and the modified hydroxide hydrogen site makes relatively little difference in the pair potential in the physically relevant region. Figure 4 shows the geometries of the solutes hydrogen bonding with a single water molecule. The carbonyl oxygen is solvated in A, B, and D while in C and E the hydroxide oxygen is solvated. In Table III, the solute TIP3P results for these configurations, in which the intermolecular variables were optimized under C_s symmetry, are compared to both ab initio and solute TIP4P results.[10] The replacement of TIP4P water by TIP3P in the present work has a small effect on these hydrogen-bonding configurations; the energy differences are less than 6% and the acceptor–hydrogen distances differ by less than 0.1 Å. In most cases, the differences between the ab initio and TIP4P results are larger than the differences between TIP4P and TIP3P.

In accord with the MC simulation,[10] the integral equation calculation was done at a temperature of 298.15 K and ρ_{H_2O} = 0.997 g/cm^3 at 1 atm. The experimental water isobaric thermal expansion coefficient $\alpha_{v,P}$ = 2.57 × 10^{-4} K^{-1} is used instead of 4.1 × 10^{-4} K^{-1} calculated from a simulation.[39] The dependence of the water dielectric constant, ϵ_0, on temperature and density are determined from experimental data.[30,40] For the temperature and pressure dependence of the water density, the equations given by Kell[41] were used.

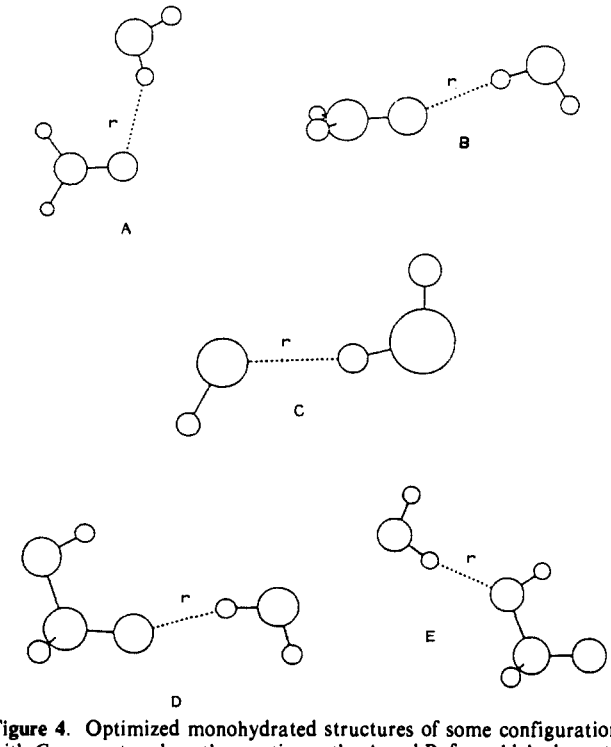

Figure 4. Optimized monohydrated structures of some configurations with C_s symmetry along the reaction path. A and B, formaldehyde–water complexes; C, hydroxide–water complex; D and E, tetrahedral complex or transition-state complex with water.

(40) Owen, B. B.; Miller, R. C.; Milner, C. E.; Cogan, H. L. *J. Phys. Chem.* **1961**, *65*, 2065.
(41) Kell, G. S. *J. Chem. Eng. Data* **1975**, *20*, 97.

3. Results and Discussions

3.1. Thermodynamics. In Table IV, the HNC–RISM results for the solvation free energy and enthalpy and the solvent reorganization energy for the reactants, the transition states, and the tetrahedral complex are given. No such absolute calculations were described by Madura and Jorgensen,[10] though they are possible by free energy simulation methods.[42] The calculated solvation free energy of −147 kcal/mol for OH^- is significantly larger than the experimental estimates of −89 to −93 kcal/mol.[43,44] In view of the success of HNC–RISM for the solvation thermodynamics of Cl^- and Br^-,[30] such a discrepancy is disappointing. If a larger Lennard-Jones radius (σ = 4.2 Å instead of 3.2) is used for the hydroxide oxygen, a value of −90 kcal/mol is obtained. The solvation enthalpy of −163 kcal/mol for OH^- is also larger than the value of −115 ± 10 kcal/mol from the experiment.[43,45] The overestimation is a result of too strong hydrogen bonding with the hydroxide oxygen in the HNC–RISM theory (see Figure 10) and appears to be a shortcoming of the theory rather than the choice of parameters. Values of −140 and −100 ± 5 kcal/mol were reported in molecular mechanics[46] and a Monte Carlo[10] calculation, respectively. For the formaldehyde, no experimental data are directly comparable due to diol formation with water.[11] The combined H_2CO and OH^- solvation enthalpy of −167 (−164 at R_{C-O2} = 7.4 Å) kcal/mol can be compared with −147 ± 13 kcal/mol from ref 10, where they are separated at R_{C-O2} = 7.4 Å.[10] For the solvent reorganization, the HNC–RISM result of 155 (152 at R_{C-O2} = 7.4 Å) kcal/mol can be compared with the value of 74 ± 13 kcal/mol from ref 10. The convergence difficulty in the solvent reorganization energy from simulations[47] makes it unclear which is more accurate.

For the transition state and the tetrahedral complex, no experimental data are available for comparison. However, they can be compared with the work of Madura and Jorgensen.[10] The solvation enthalpies of −120 and −117 kcal/mol from the HNC–RISM theory can be compared with −79 ± 12 and −70 ± 11 kcal/mol from the MC simulation for the transition state and the tetrahedral complex, respectively (see Table IV). The absolute values differ significantly while the relative value of 3 kcal/mol from the HNC–RISM is well within the uncertainty of 9 ± 16 kcal/mole from ref 10. Better agreement for solvation enthalpies was found with the molecular mechanics calculation of a similar reaction, $OH^- + HCONH_2$,[46] in which they were estimated from energy-minimized configurations for the solutes in TIP3P water. However, the absolute solvent reorganization energies also disagree significantly (see Table IV); only the trend in going from the tetrahedral complex to the reactant is similar.

The free energy [potential of mean force, i.e., the sum of $U(r)$ and $\Delta\mu^{(o)}_{u,sol}$], relative to the infinitely separated reactants, for the $OH^- + H_2CO$ reaction in TIP3P water is given as the thick solid line in the upper panel of Figure 1. The open circles with error bars correspond to averages from two MC simulations.[10] The solutes are assumed to be rigid, so motional contributions to the free energy are not included. The qualitative agreement with the MC results is very good. Overall there is an essential change in the reaction profile, relative to the gas phase. The latter has a shallow well for a charge–dipole interaction at R_{C-O2} = 2.74 Å and a deep well at 1.47 Å upon the formation of the tetrahedral complex. By contrast, in water the tetrahedral complex is a deep but metastable minimum; i.e., it is less stable than the reactants. The position of the transition state is predicted to shift from R_{C-O2} = 2.39 Å in the gas phase to 2 Å in water, in agreement with the MC result, and is similar to the case of the $OH^- + HCONH_2$ reaction.[46] Two small shoulders were found at R_{C-O2} = 2.4 and

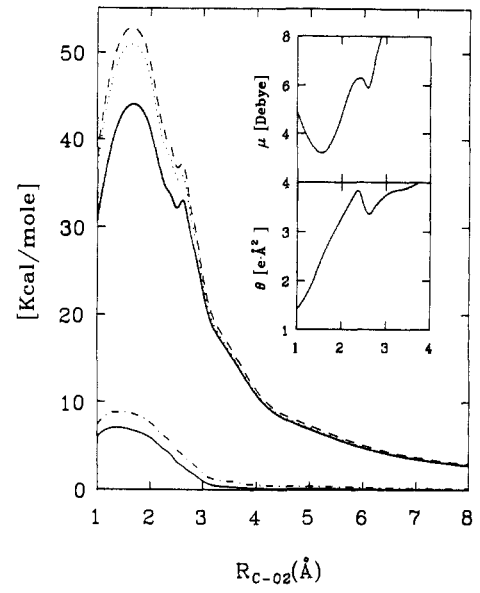

Figure 5. Solvent contribution to the energy profile for the $OH^- + H_2CO$ reaction. (—) $\Delta\mu^{(o)}_{u,sol}(r)$; (···) $\Delta h^{(o),T}_{u,sol}(r)$; (- - -) $\Delta h^{(o),\theta}_{u,sol}(r)$; (—) $T\Delta s^{(o),T}_{u,sol}(r)$; (-·-) $T\Delta s^{(o),\theta}_{u,sol}(r)$. Inset: Upper panel, the dipole moment (μ) with the coordinate origin at the carbonyl carbon; lower panel, the quadrupole moment (θ) with the center of charge as the origin.

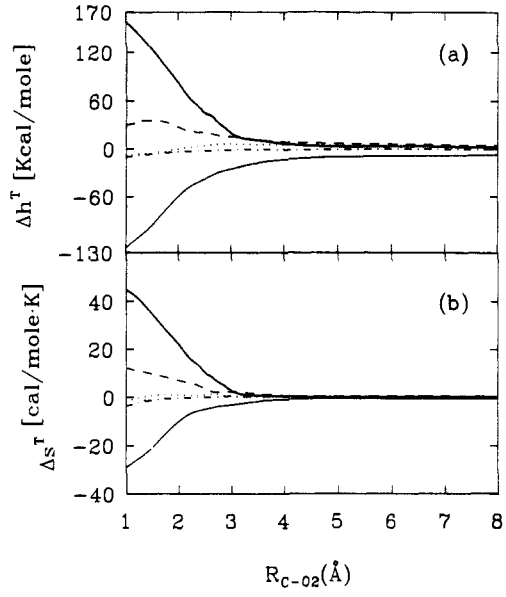

Figure 6. Site decomposition of the solvation thermodynamics. (—) O2; (-·-) H2; (- - -) C; (···) H1; (—) O1. (a) Enthalpy. (b) Entropy.

2.6 Å. They are also present in the MC profile. Since the MC results have sizable statistical error bars,[10] the presence of the shoulders in the HNC–RISM profile, which has no statistical error, suggests that they are real, at least for this particular choice of parameters. The deep minimum at R_{C-O2} = 1.47 Å reflects the formation of covalent bond in the gas phase. To focus on the difference between gas-phase and solution profiles, we of a the solvation free energy contribution in Figure 5 as the thick solid line. The solvation is most unfavorable at $R_{C-O2} \approx 1.7$ Å, near the point at which charges on the hydroxide and carbonyl oxygens are approximately equal (see Table II), instead of at 2 Å, the apparent transition state in water. This result is consistent with a Born solvation model,[48] since the solvation free energy varies as the square of the charge.

The presence of a barrier at R_{C-O2} = 1.7 Å and a shoulder near 2.6 Å can be qualitatively understood by considering the charge distribution in the solute. Since the total charge of the solute

(42) Jorgensen, W. L.; Buckner, J. K.; Boudon, S.; Tirado-Rives, J. *J. Chem. Phys.* **1988**, *89*, 3742.
(43) Friedman, H. L.; Krishnan, C. V. In *Water: A Comprehensive Treatise*; Franks, F., Ed.; Plenum Press: New York, 1973; Vol. 3, p 1.
(44) Gomer, R.; Tyson, G. *J. Chem. Phys.* **1977**, *66*, 4413.
(45) Arshadi, M.; Kebarle, P. *J. Phys. Chem.* **1970**, *74*, 1483.
(46) Weiner, S. J.; Singh, U. C.; Kollman, P. A. *J. Am. Chem. Soc.* **1985**, *107*, 2219.
(47) Tidor, B.; Karplus, M., to be published.
(48) Roux, B.; Yu, H. A.; Karplus, M. *J. Phys. Chem.*, in press.

Table V. Water Oxygen Site Coordination Numbers of Carbonyl and Hydroxide Oxygens[a]

R_{C-O2}, Å	MC[b]			MD[c]			HNC-RISM[c]		
	O1–O_w	O2–O_w	sum	O1–O_w	O2–O_w	sum	O1–O_w	O2–O_w	sum
∞	1.7	6.3	8.0	2.4	6.7	9.1	3.5	5.4	8.9
2.00	3.6	4.3	7.9	3.4	3.9	7.3	3.7	3.7	7.4
1.47	4.7	3.2	7.9	4.6	3.0	7.6	4.2	2.8	7.0

[a] The integration cutoffs are 3.4 Å for O2–O_w and 3.2 Å for O1–O_w. [b] Monte Carlo simulation with TIP4P;[10] the reactants are at R_{C-O2} = 7.4 Å. [c] Molecular dynamics simulation and HNC-RISM with TIP3P.

remains constant at −1, all higher multipoles depend on the choice in the origin of the coordinate frame for the multipole expansion. We choose the origin to be the carbonyl carbon, the site of nucleophilic attack. The calculated solute dipole moment, μ, as a function of the reaction coordinate is shown in the upper panel of the inset in Figure 5. The solvent contribution to the reaction profile correlates well with the strength of the solute dipole moment. The first dipole minimum is near R_{C-O2} = 1.7 Å, the position of the major barrier in the solvation free energy (Figure 5). The second minimum is near R_{C-O2} = 2.6 Å, at which there is a rapid change in the angle O1–C–O2.[10] A reduction in the solute dipole moment decreases the solute–solvent interaction energy and leads to a barrier in the solvation enthalpy. Conversely, it leads to a favorable solvation entropy due to less restriction on the orientational degrees of freedom of the surrounding water molecules. Since the magnitude of the enthalpy is larger than the entropy, a barrier in the solvation free energy results.

To examine the origin of the shoulder at R_{C-O2} = 2.6 Å, we choose the center of the solute charges as the coordinate origin for the multipole expansion. In this case, the first nonzero multipole (other than the monopole) is the solute quadrupole moment, θ. The quadrupole terms for the solute as a function of the reaction coordinate is calculated from a principle axis transformation followed by construction of the equivalent ideal quadrupoles.[49] That is, for each solute at the given reaction coordinate, the quadrupole tensor with respect to its center of charge is diagonalized and the strength of the quadrupole moment is calculated by summing the absolute magnitude of the largest and the smallest eigenvalues.[49] The result is shown in the lower panel of the inset in Figure 5. The local minimum near 2.6 Å reflects a change in the direction of approach of the hydroxyl relative to the formaldehyde; the angles O···C=O and H—O···C change from 180° at R_{C-O2} = 2.74 Å to 168 and 173° respectively, near R_{C-O2} = 2.6 Å (see Table III of ref 10). This abrupt geometric variation was reported to cause difficulty in the MC simulation and was overcome by close spacings in the umbrella sampling scheme.[10] The local maximum at R_{C-O2} = 2.4 Å is near the transition state in the gas phase.

Although the overall features of the free energy profiles from integral equation theory and the Monte Carlo simulation are similar, there are quantitative differences. The 21 kcal/mol activation free energy from the present study is somewhat smaller than the value of 24–28 kcal/mol obtained from the MC simulation.[10] A still smaller barrier (19 kcal/mol) is obtained if no dielectric constant correction is used, i.e., if A = 1 is used in eq 4 instead of A = 0.959. The calculated barrier is close to the experimental value of 15–19 kcal/mol activation free energy for alkaline hydrolysis of esters[50] and values of 22–24 kcal/mol for amides[51] but is significantly larger than the estimate of 9 kcal/mol for formaldehyde.[52,53] To obtain a value of the activation free energy, the simple gas-phase formula[52,53] for the rate constant k_f

$$k_f = \left(\frac{k_B T}{h}\right) \exp\left(-\frac{\Delta G^*}{k_B T}\right) \qquad (14)$$

was used, where h is the Planck's constant in this equation. The experimental value of k_f was obtained by the analysis of a complex reaction scheme and measurements at a single temperature. Equation 14 is not generally applicable in solution due to the neglect of dynamic effects (e.g., barrier recrossing, temperature dependence of viscosity),[54] and because it does not include the possible formation of a preequilibrium caged complex;[55] i.e., A + B ⇌ A–B → A′–B′, where A–B is the ion–dipole complex and A′–B′ represents the transition state. Introduction of a complex with parameters corresponding to the minimum at R_{C-O2} = 4.3 Å in Figure 1 leads to a correction of eq 14 by an order of magnitude, not sufficient to significantly improve the agreement between theory and experiment. The large difference suggests that a new determination of the reaction rate, including measurements as a function of temperature, would be of interest.

The tetrahedral complex is lower by 13 kcal/mol than the transition state in the HNC–RISM calculation, in agreement with 10–14 kcal/mol in the MC simulation.

One possible source of the higher barrier from the MC simulation is the difference in the water models. The TIP4P used in the MC study has a partial charge on the hydrogen sites that is 25% larger than that of the TIP3P although its dipole moment is smaller by 8%. The interaction energy for the reactant hydroxide anion with a single TIP4P water molecule is more favorable by −0.8 kcal/mol than with a single TIP3P water (see Table III). By contrast, the interaction of the transition state with a single TIP4P water is less favorable by 0.8 kcal/mol than with a TIP3P water (see Table III). This 1.6 kcal/mol increase in the barrier in TIP4P is consistent with a higher barrier in the MC simulation, compared with the HNC–RSM theory. A distinct feature in the PMF from HNC–RISM theory is the existence of a global minimum (−0.8 kcal/mol) at R_{C-O2} = 4.3 Å. The statistical uncertainty in MC simulations prevents the finding of such a shallow minimum.[10] The separation of 4.3 Å is smaller (by 1.7 Å) than that appropriate for a fully solvent-separated ion–dipole intermediate, so the minimum is a result of delicate balance between the attractive $U(r)$ and the repulsive $\Delta\mu^{(o)}_{\mu,sol}(r)$ in this region.

To obtain a more detailed analysis of the solvation, we decompose the solvent contribution to the free energy profile from each solute site and plot them as a function of the reaction coordinate; the possibility of such a decomposition follows directly from the form of eq 6. The results are shown in Figure 3b. The excellent correlation with the trend in the charge transfer (Figure 3a) makes clear that electrostatic effects are dominant. The correlation is consistent with the charge dependence of the solvation free energy for monatomic solutes in water.[29,48] The contribution (relative to reactants) to the transition state at R_{C-O2} = 2 Å from the hydroxide and the carbonyl oxygens are 76 and −56.5 kcal/mol, respectively (see Table IV). The data reflect desolvation at the hydroxide oxygen and increased solvation of the carbonyl oxygen as the charge is being transferred from one to the other (see Figures 3, 7, and 8 and Table V). Their combined contribution is 19.5 kcal/mol compared with the total of 41 kcal/mol; the major part of the difference comes from the carbonyl carbon, which contributes 25 kcal/mol (see Table IV and Figure 3b). The latter results from the fact that the strong interaction between water and the hydroxide and carbonyl oxygens

(49) Bottcher, C. J. F. *Theory of Electric Polarization*; Elsevier: New York, 1973; Vol. I, Chapter 1.
(50) Guthrie, J. P. *J. Am. Chem. Soc.* **1973**, *95*, 6999.
(51) Guthrie, J. P. *J. Am. Chem. Soc.* **1974**, *96*, 3609.
(52) Guthrie, J. P. *J. Am. Chem. Soc.* **1978**, *100*, 5892.
(53) Jorgensen, W. L. *Adv. Chem. Phys.* **1988**, *70*, Part 2, 469.
(54) Bergsma, J. P.; Gertner, B. J.; Wilson, K. R.; Hynes, J. T. *J. Chem. Phys.* **1987**, *86*, 1356.
(55) Amdur, I.; Hammes, G. G. *Chemical Kinetics: Principles and Selected Topics*; McGraw-Hill: New York, 1966; Chapters 2, 5.

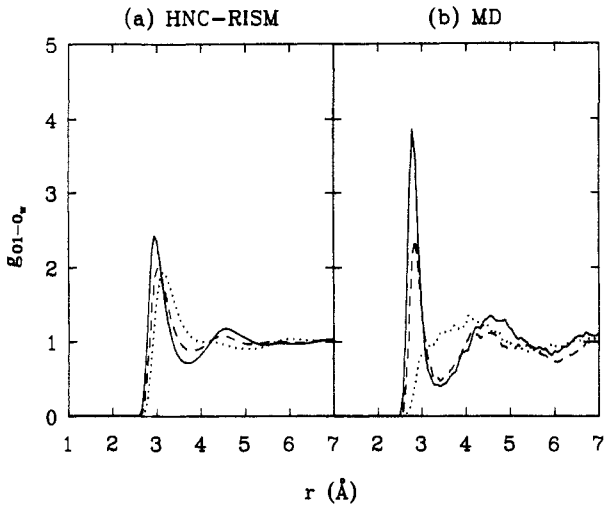

Figure 7. Carbonyl oxygen, O1, and water oxygen, O_w, radial distribution functions. (···) $R_{C-O2} = \infty$; (- - -) $R_{C-O2} = 2$ Å; (—) $R_{C-O2} = 1.47$ Å. (a) HNC-RISM. (b) MD simulation.

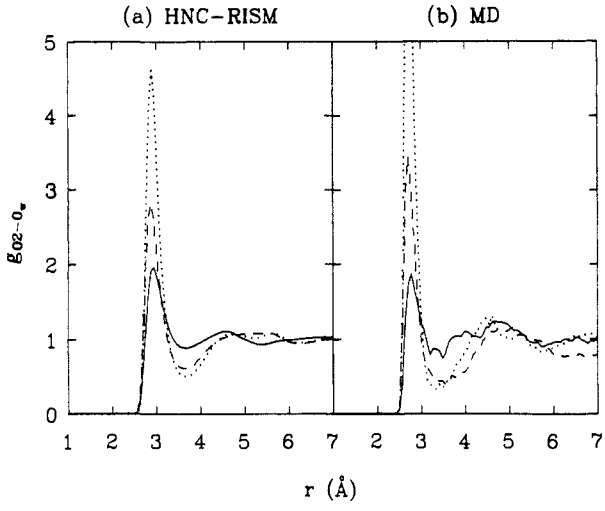

Figure 8. Hydroxide oxygen, O2, and water oxygen, O_w, radial distribution functions. (···) $R_{C-O2} = \infty$; (- - -) $R_{C-O2} = 2$ Å; (—) $R_{C-O2} = 1.47$ Å. (a) HNC-RISM. (b) MD simulation.

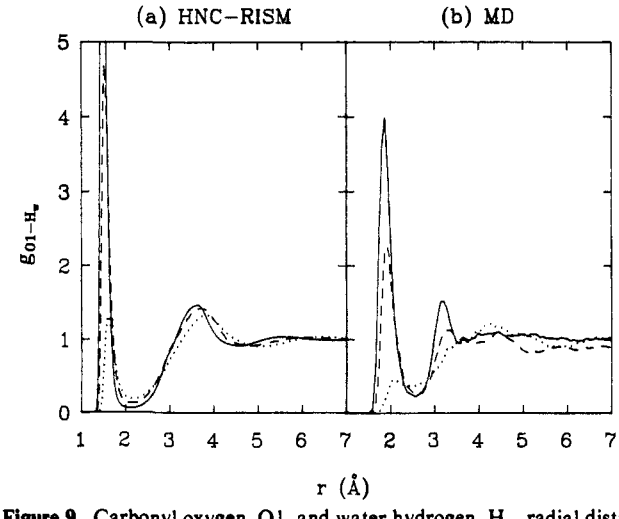

Figure 9. Carbonyl oxygen, O1, and water hydrogen, H_w, radial distribution functions. (···) $R_{C-O2} = \infty$; (- - -) $R_{C-O2} = 2$ Å; (—) $R_{C-O2} = 1.47$ Å. (a) HNC-RISM. (b) MD simulation.

brings water hydrogens near the carbonyl carbon (see Figures 12 and 13). Therefore, despite the structural shielding of carbonyl

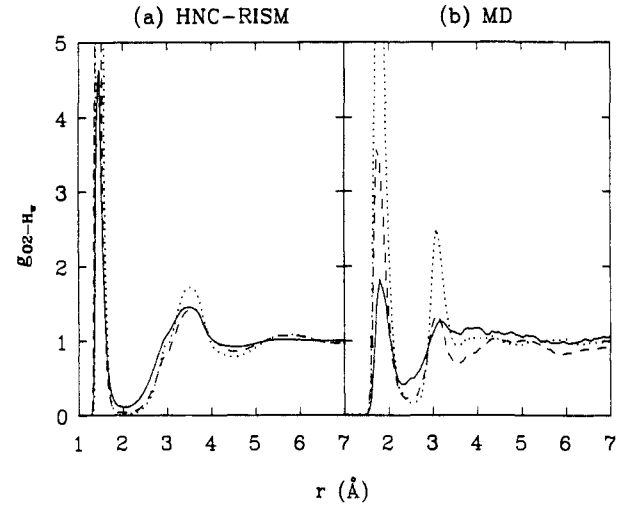

Figure 10. Hydroxide oxygen, O2, and water hydrogen, H_w, radial distribution functions. (···) $R_{C-O2} = \infty$; (- - -) $R_{C-O2} = 2$ Å; (—) $R_{C-O2} = 1.47$ Å. (a) HNC-RISM. (b) MD simulation.

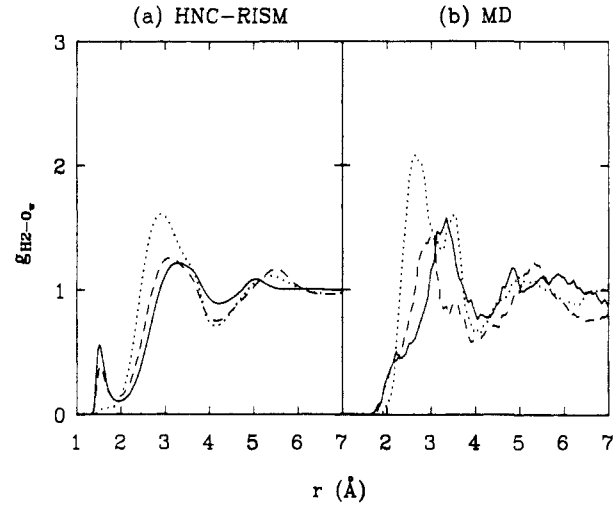

Figure 11. Hydroxide hydrogen, H2, and water oxygen, O_w, radial distribution functions. (···) $R_{C-O2} = \infty$; (- - -) $R_{C-O2} = 2$ Å; (—) $R_{C-O2} = 1.47$ Å. (a) HNC-RISM. (b) MD simulation.

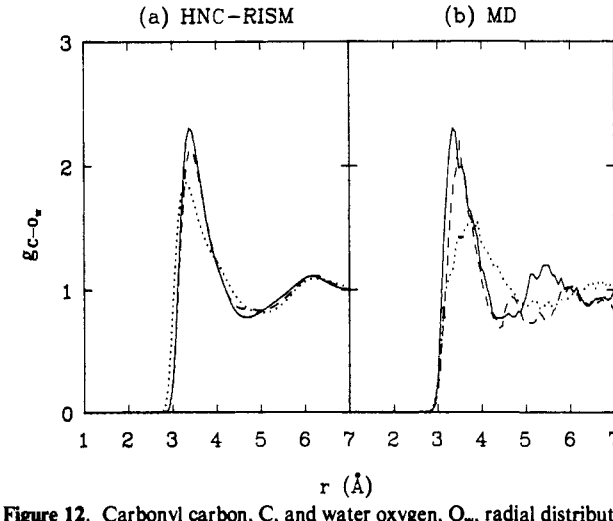

Figure 12. Carbonyl carbon, C, and water oxygen, O_w, radial distribution functions. (···) $R_{C-O2} = \infty$; (- - -) $R_{C-O2} = 2$ Å; (—) $R_{C-O2} = 1.47$ Å. (a) HNC-RISM. (b) MD simulation.

carbon (a 30% reduction in the accessible surface area with a spherical probe of radius 1.425 Å based on the algorithm of Lee and Richards[56]) in the transition state and the tetrahedral complex,

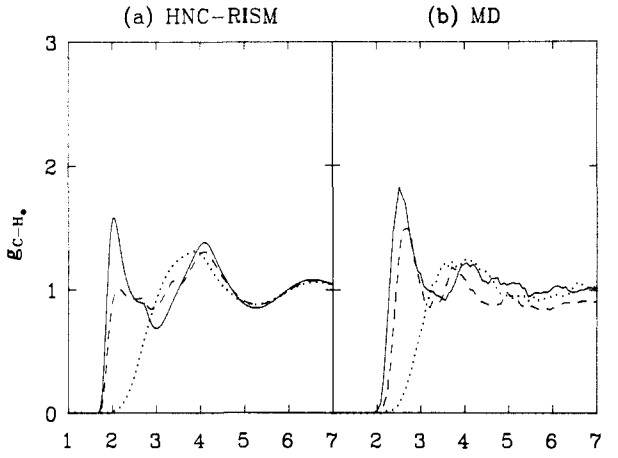

Figure 13. Carbonyl carbon, C, and water hydrogen, H_w, radial distribution functions. (···) $R_{C\text{-}O2} = \infty$; (---) $R_{C\text{-}O2} = 2$ Å; (—) $R_{C\text{-}O2} = 1.47$ Å. (a) HNC-RISM. (b) MD simulation.

it plays a significant role in the thermodynamics.

In addition to the free energy of solvation, its enthalpic and entropic components were calculated; the result is shown in Figure 1, upper panel. The dotted ($\Delta h^{(o),T}_{u,sol}$, ···) and the dashed ($\Delta h^{(o),\rho}_{u,sol}$, ---) lines are enthalpies calculated by temperature (eqs 11 and 12) and density (eqs 11 and 13) derivatives, respectively. The corresponding entropies from temperature and density derivatives are given as the thin solid ($T\Delta s^{(o),T}_{u,sol}$, —) and the dash-dotted ($T\Delta s^{(o),\rho}_{u,sol}$, -·-) lines. The results show that the enthalpy determines the free energy profile in water, as well as in the gas phase. The enthalpy barrier of 26–28 kcal/mol is smaller than the rather uncertain value (given as 68 ± 29 kcal/mol) from ref 10 and is larger than the estimate of 22 kcal/mol for the $OH^- + HCONH_2$ reaction.[46] The two different thermodynamic derivatives lead to a mismatch in enthalpy (or entropy) of ~2 kcal/mol; this provides one measure of the errors in the approximate integral equation theory.

The solvation contribution to enthalpy and entropy is given in Figure 5. As in Figure 1, the enthalpy dominates in the solvation and the entropy variations are smaller and smoother in comparison. This behavior is consistent with the result for monatomic ions in water.[29] The decomposition into enthalpy and entropy contributions from individual sites calculated from the isobaric temperature derivatives of the free energy (eqs 11 and 12)[30] is given in Figure 6a and b as a function of the reaction coordinate. The correlation with the trend in charge transfer (Figure 3a) is similar to that for the solvation free energy. Of the total solvent-induced enthalpy barrier of 47 kcal/mol (relative to the reactants) at $R_{C\text{-}O2}$ = 2 Å, the contributions from hydroxide oxygen, carbonyl oxygen, and carbonyl carbon are 82.6, −59.5, and 27.3 kcal/mol, respectively (see Table IV).

3.2. Distribution Functions. In this section, the radial distribution functions calculated from the HNC-RISM theory are compared with those from molecular dynamics (MD) simulations using the same potentials; corresponding radial distribution functions are given in Figures 7–12 of ref 10. In general, the HNC-RISM theory overestimates the electrostatic interactions and leads to lower peaks in g_{--} (e.g., $g_{O1\text{-}Ow}$ and $g_{O2\text{-}Ow}$ in Figures 7 and 8) and higher peaks in g_{-+} (e.g., $g_{O1\text{-}Hw}$ and $g_{O2\text{-}Hw}$ in Figures 9 and 10) compared with the MD simulation.

In Figures 7 and 8, the pair distribution functions for the carbonyl and water oxygens (O1–O_w) and the hydroxide and water oxygens (O2–O_w) from HNC-RISM theory and the MD simulation are given. Other than $g_{O1\text{-}Ow}$ for formaldehyde (Figure 7, ···), HNC-RISM and MD give similar distribution functions. This is particularly true in terms of the trends in going from the reactants (···) through the transition state (---) to the tetrahedral complex (—). Quantitatively, the HNC-RISM theory predicts first peak positions 0.1 Å larger and peak heights from 0.5 to 3 smaller than the MD simulation; the latter, which occurs for $g_{O2\text{-}Ow}$, is a significant discrepancy. In the case of $g_{O1\text{-}Ow}$ for the formaldehyde, the HNC-RISM theory showed a first peak at 3.1 Å that is absent in the MD simulation. This results from a stronger hydrogen-bonding peaks in the HNC-RISM $g_{O1\text{-}Hw}$ as compared with that from the MD simulation (see Figure 9). The positions of the hydrogen-bonding peaks too close to the origin (Figures 9a, 10a, and 11a) is a characteristic defect in the HNC-RISM integral equation theory.[14,29]

In comparing $g_{O1\text{-}Ow}$ and $g_{O2\text{-}Ow}$ with those from the MC simulation of Madura and Jorgensen,[10] the MD simulation gave similar peak positions but generally smaller (~0.5) peak heights, except for the reactants. In Table V, the coordination numbers of water oxygen around the carbonyl and the hydroxide oxygens are listed. All data show transfer of water coordination from the hydroxide oxygen to the carbonyl oxygen along the reaction path as a consequence of the charge transfer between the two oxygens. Both MD and HNC-RISM data indicate that the reactant is solvated by one to two more water molecules than the transition state and the tetrahedral complex, in contrast to the MC data in which the total number of coordinated waters remain equal to eight. The discrepancy between the MD and MC simulations for the reactants may be due partly to the fact that the MD simulation was done with two separate H_2CO and OH^- simulations whereas the MC was done with the two reactants at $R_{C\text{-}O2}$ = 7.4 Å in a single simulation. In the presence of the more favorably solvated OH^-, there is less water available to solvate the H_2CO; in MC the water oxygen coordination number for the carbonyl oxygen is 1.7 compared with 2.4 in MD (see Table V). This raises the question of whether a separation of $R_{C\text{-}O2}$ = 7.4 Å is large enough to model the infinitely separated reactants. An explicit HNC-RISM calculation at $R_{C\text{-}O2}$ = 7.4 Å gave a solvent contribution to the free energy profile of 3.3 kcal/mol, relative to the infinitely separated reactants; the contribution is reduced to 1.3 kcal/mol at $R_{C\text{-}O2}$ = 12 Å. By choosing $R_{C\text{-}O2}$ = 7.4 Å (instead of at infinite separation) as the reactant in the HNC-RISM calculation, the activation free energy is lowered from 21 to 17.7 kcal/mol. The comparison also raises the possibility that the free energy barrier in water is induced by reduction both in the number of hydrogen bonds and in their strength. Proximity analysis[57] of the MC simulation data led to numbers of first shell water equal to 9.8, 7.9, and 8.6 for the reactants, transition state, and tetrahedral complex, respectively.[10] Of them, 6.3, 5.1, and 5.8 can be assigned as waters coordinating the hydroxide moiety and carbonyl oxygn in the reactants, the transition state, and the tetrahedral complex, respectively.

The rather different $g_{O1\text{-}Ow}$ from the HNC-RISM theory and the MD simulation for the reactant (Figure 7, ···) leads to different coordination numbers. In the HNC-RISM, there are 3.5 water oxygens around the carbonyl oxygen, more than the 2.4 in the MD simulation. On the other hand, the hydroxide oxygen has a water oxygen coordination number of 6.7 in the MD simulation, more than 5.4 in the HNC-RISM; it is 6.3 in the MC simulation.[10] The individual discrepancies for reactants cancel each other to give the apparent agreement of total reactant water oxygen coordination number of 9.1 in MD and 8.9 in HNC-RISM. The coordination numbers for the transition state and the tetrahedral complex from HNC-RISM and the MD simulation are in good agreement.

In Figures 9 and 10, the radial distribution functions between the water hydrogen and the carbonyl oxygen (O1–H_w) and the hydroxide oxygen (O2–H_w) from the HNC-RISM theory and the MD simulation are given. Agreement on qualitative trends exists between the two sets of distribution functions. Quantitatively, the first hydrogen-bonding peaks from HNC-RISM theory

(56) Lee, B.; Richards, F. M. *J. Mol. Biol.* **1971**, *55*, 379. The radius of 1.425 Å is half of the position, 2.85 Å, of the first peak in water oxygen–oxygen radial distribution function, g_{OO}. The surface algorithm implemented in the program CHARMM was used.

(57) Mehrotra, P. K.; Beveridge, D. L. *J. Am. Chem. Soc.* **1980**, *102*, 4287.

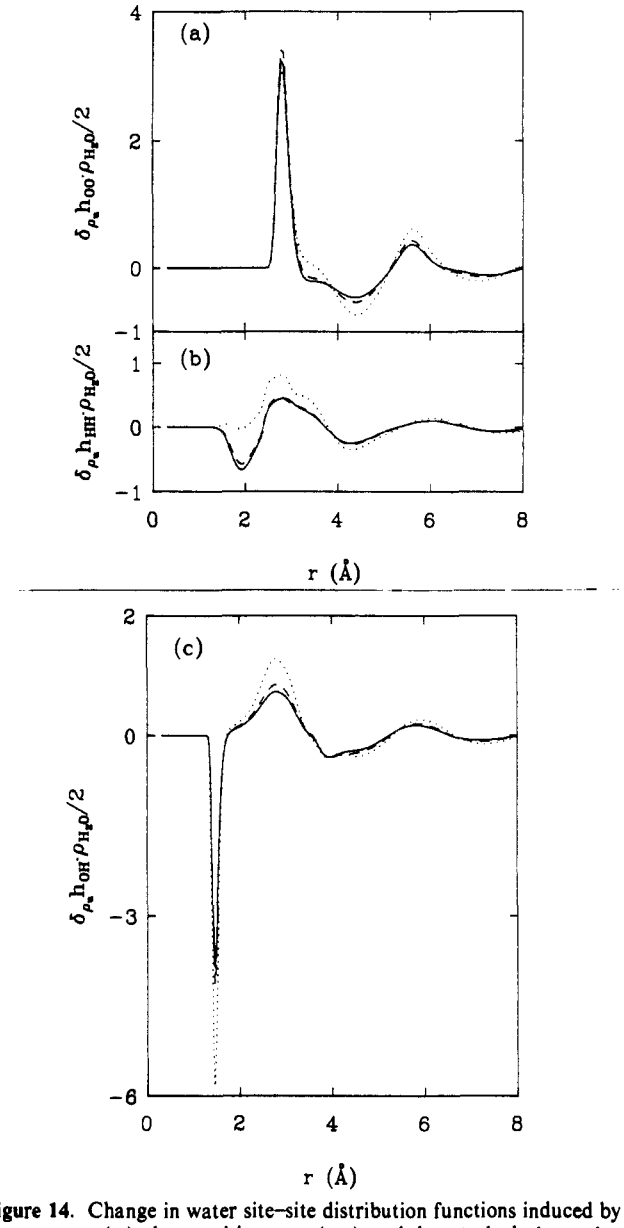

Figure 14. Change in water site–site distribution functions induced by the reactants (···), the transition state (---), and the tetrahedral complex (—). (a) $\delta_{\rho_u} h_{OO}$. (b) $\delta_{\rho_u} h_{HH}$. (c) $\delta_{\rho_u} h_{OH}$.

are positioned 0.4 Å closer to the origin and have much greater heights; the second peaks in turn are positioned slightly further with smaller heights. The distribution functions from the MD simulation have smaller peak heights than the MC simulation[10] except in the case of the hydroxide reactant (Figure 10, ···), where the MD simulation has a higher hydrogen-bonding peak.

In Figure 11, the pair distribution functions between hydroxide hydrogen and water oxygen (H2–O_w) from the HNC–RISM theory and the MD simulation are given. For the hydroxide reactant (···), the feature of a double peak in the MD $g_{H2\text{-}Ow}$ shows up as a first peak plus a shoulder in the HNC–RISM distribution function. In contrast, the hydrogen-bonding peak at 1.5 Å for the transition state and the tetrahedral complex in the HNC–RISM $g_{H2\text{-}Ow}$ are present only as small shoulders near 2.2 Å in the MD distribution functions. If a σ_{H2} larger than 0.4 Å is used, these two peaks move out to larger r to give better agreement between the HNC–RISM and the MD. In the MC simulation,[10] a distinct hydrogen-bonding peak is present in $g_{H2\text{-}Ow}$ at 2 Å for the tetrahedral complex.

In Figure 12, the pair distribution functions between the carbonyl carbon and water oxygen (C–O_w) from the HNC–RISM theory and the MD simulation are shown. Except for the reactant (···), the HNC–RISM and MD $g_{C\text{-}Ow}$ are similar, especially the first peak positions and heights; the second peaks are either less developed or at a larger distance in the HNC–RISM than in the MD simulation. For the formaldehyde reactant, the HNC–RISM theory gave a closer and larger solvation shell than the MD simulation; this is similar to that of the formaldehyde oxygen [see Figure 7 (···) and Table V]. By comparison with the MC simulation[10] in which the $g_{C\text{-}Ow}$ for the reactant is rather featureless, the present MD $g_{C\text{-}Ow}$ are more structured with a distinct first solvation peak at 3.8 Å of height 1.5. This difference is similar to the reactant carbonyl and hydroxide oxygens solvation mentioned above.

In Figure 13, the pair distribution functions for the carbonyl carbon and water hydrogen (C–H_w) from the HNC–RISM theory and the MD simulation are shown. There is good qualitative agreement and the increase in water hydrogen coordination around the carbonyl carbon in the transition state (---) and the tetrahedral complex (—) is very clear. This has the thermodynamic consequence of a significant repulsive solvation free energy contribution from the carbonyl carbon site, as discussed above.

It is interesting to determine how the structure of the solvent changes along the reaction path. In Figure 14, the average change in the water site–site distribution functions induced by the reactant, the transition state, and the tetrahedral complex are given; they were calculated from eqs 9 and 10 and scaled by $\rho_{H_2O}/2$.[29] The results for the transition state (---) and the tetrahedral complex (—) are typical of the water structural modification induced by an atomic anion.[29] The introduction of solute increases the effective density of water and leads to an increase in the first OO peak as seen in $\delta_{\rho_u} h_{OO}$. There is a decrease in the first hydrogen site correlation peak, as seen in $\delta_{\rho_u} h_{HH}$ and $\delta_{\rho_u} h_{OH}$, since the overall negatively charged solute tends to compete with the water molecules for the positively charged hydrogens. The case of the reactant can be viewed as weighted sums of changes induced by an anion (OH^-) and a neutral solute (H_2CO).[29]

The changes in solvent structure result in a reorganization contribution to the enthalpy that is positive in all cases. Since it is largest for the separated reactants, the solvent reorganization energy contributes (relative to the reactant) −44 and −47 kcal/mol to the solvation enthalpy for the transition state and the tetrahedral complex, respectively. Values of −41 and −44 kcal/mol are obtained, respectively, if the reactants are separated at $R_{C\text{-}O2}$ = 7.4 Å. There is, however, a cancellation of this in the PMF due to a corresponding term in the entropy.[29] The MC simulation[10] reported solvent reorganization energies of 2 ± 18 and 10 ± 17 kcal/mol for the transition state and the tetrahedral complex relative to the reactants at $R_{C\text{-}O2}$ = 7.4 Å (see Table IV). However, these values are too uncertain to make a meaningful comparison with the HNC–RISM results. Values of −31 kcal/mol with no error estimates were reported for the OH^- + $HCONH_2$ reaction.[46]

4. Conclusions

The HNC–RISM integral equation theory has been used to study the effect of solvation on the nucleophilic addition of OH^- to H_2CO. In accord with a Monte Carlo simulation, it is found that the deep attractive well found in the gas-phase calculation of the reaction path is replaced by a large barrier in aqueous solution. The overall features of the free energy profiles from the HNC–RISM theory and the MC simulation are in good agreement. Quantitatively, the HNC–RISM free energy barrier is 19 (without dielectric correction) and 21 kcal/mol (with dielectric correction) as compared with 24–28 kcal/mol from the MC simulation. The experimental estimates are 15–19 kcal/mol for esters, 22–24 kcal/mol for amides, and only ~9 kcal/mol for formaldehyde. The source of the disagreement for formaldehyde is not clear, though complications in the integration of the experimental data may play a role. Both the microscopic mechanism of the solution reaction and dynamic effects should be considered.[54,55]

One advantage of the analytical integral equation theory relative to simulations in free energy calculations is the absence of statistical error. This makes it possible to obtain precise results that confirm some detailed features of the reaction profile that are at

the level of statistical uncertainties in the MC simulation data; e.g., the shoulders at R_{C-O2} = 2.4 and 2.6 Å. Also in accord with the MC results, the HNC-RISM theory predicts a shift of the transition state from R_{C-O2} = 2.39 Å in the gas phase to 2 Å in water. Another advantage of the HNC-RISM theory is that temperature and density derivatives can be used to decompose the free energy into enthalpic and entropic contributions. It shows that the enthalpy provides the dominant solvent effect.

It is important to note also that the HNC-RISM calculation requires ~2 orders of magnitude less computer time than the MC simulation; an equivalent of 180 days of VAX 11/780 time was needed for the latter. Therefore, it seems clear that, given a set of quantum mechanical potentials (which are themselves vey time consuming to determine by ab initio methods, particularly for reactions), it is desirable to employ the analytic integral equation theory to make a preliminary exploration of the reaction mechanism in aqueous solution or do other more extensive searches of the conformational space that are not possible by simulations. Moreover, the HNC-RISM free energy profiles can provide guidelines for the construction of a biasing function for the umbrella sampling scheme used in simulation studies.

A disadvantage of the HNC-RISM theory is that it is approximate, even for a given set of parameters, and that there are possible inaccuracies in the results. In the present case, molecular dynamics simulations with the same model potential show some quantitative deficiencies in the radial distribution functions from the HNC-RISM theory. The accuracy of the thermodynamic values for the reaction path presumably involves some cancellation of errors. In part, this is due to the fact that differences in rather than absolute values of the solvation free energy are used. However, the nature of the error cancellation is not fully understood, so that it is not yet possible to predict a priori when the HNC-RISM theory can be applied with confidence. Experience from a number of studies, including the present one, suggests that it is best for polar or charged solutes with net charge no larger than unity. More studies are needed to clarify the situation. Also it would be useful to have better closures that retain the simplicity of the HNC-RISM calculations while at the same time improve the accuracy of the thermodynamic and structural results.[58]

Acknowledgment. We thank Dr. Jiin-yun Liang for contributing to our interest in this system. We also thank Drs. Jiali Gao and Jiin-yun Liang for helpful discussions. This research was supported in part by a grant from the National Science Foundation.

Registry No. OH^-, 14280-30-9; H_2CO, 50-00-0.

(58) Roux. B.; Karplus, M.; Chandler, D., submitted.

Free Energy of Association of the 18-Crown-6:K^+ Complex in Water: A Molecular Dynamics Simulation

Liem X. Dang and Peter A. Kollman*

Contribution from the Department of Pharmaceutical Chemistry, School of Pharmacy, University of California, San Francisco, California 94143. *Received November 3, 1989*

Abstract: We study a cation–crown association process in aqueous solution, using thermodynamic perturbation theory[1] and molecular dynamics simulations. The process studied is the association of K^+ with 18-crown-6. The results obtained in these simulations give both structural and energetic insight. The potential of mean force for the association of K^+ to 18-crown-6 in water displays a minimum significantly different from the crystal structure. This result can be rationalized by the greater solvation of K^+ in this configuration, compared to the crystal structure. The structures of 18-crown-6 during the dynamics simulations were studied by examining the values of the dihedral angles; the structure is in the D_{3d} conformation found in the crystal when the K^+ is in the center of the crown. However, at K^+ distances greater ~1 Å from the center of the crown, the crown changes conformation and remains in a relatively high energy (~5 kcal/mol higher internal energy than D_{3d}) conformation throughout the rest of the simulation. The calculated ΔG_b for the association of the complex in water is −3.5 ± 0.4 kcal/mol, in good agreement with the experimental value of −2.9 kcal/mol.

I. Introduction

One of the recent exciting developments in computational chemistry has been the ability to calculate free energies for complex processes in solution. These include the application of free-energy perturbation methods to study solvation,[2] enzyme catalysis,[3] and ligand binding.[4] This approach typically is used to compare properties, e.g., the relative solvation or binding free energy of two molecules.

On the other hand, it is well-known that one can calculate the free energy as a function of coordinate or potentials of mean force (PMF), and applications of the latter approach have been extremely interesting as well. A knowledge of the PMF allows one to examine in detail the effect of solvent on the solute–solute or ion–ion interactions, and to determine various thermodynamic properties such as the location of the barrier height, the equilibrium constant, and the binding free energy. Many of these properties can be compared directly to experimental measurements. These calculations are typically even more time consuming than the free-energy perturbation calculations because one is attempting to calculate the relative free energy over a large range of coordinates. The PMF's of two ions,[5] two Lennard-Jones solutes,[6] two amides,[7] or two nucleic acid bases[8] in water have been de-

(1) (a) Kirkwood, J. G. *J. Chem. Phys.* **1935**, *3*, 300. (b) Zwanzig, R. W. *J. Chem. Phys.* **1954**, *22*, 1420. Valleau, J. P.; Torrie, G. M. *Modern Theoretical Chemistry*; Berne, B. J., Ed.; Plenum Press: New York, 1977; Vol. 5, pp 169–194.

(2) Mazor, M. H.; McCammon, J. A.; Lybrand, T. P. *J. Am. Chem. Soc.* **1989**, *111*, 55. Bash, P. A. Singh, U. C.; Langridge, R.; Kollman, P. A. *Science* **1987**, *236*, 564. Warshel, A.; Sussman, F.; King, G. *Biochemistry* **1986**, *25*, 368.

(3) Rao, S. N.; Singh, U. C.; Bash, P. A.; Kollman, P. A. *Nature* **1987**, *328*, 55. Hwang, J.-K.; Warshel, A. *Biochemistry* **1987**, *26*, 2673.

(4) Lybrand, T. P.; McCammon, J. A.; Wipff, G. *Proc. Natl. Acad. Sci. U.S.A.* **1986**, *83*, 833.

(5) (a) Berkowitz, M.; Karim, O. A.; McCammon, J. A.; Rossky, P. J. *Chem. Phys. Lett.* **1984**, *105*, 577. (b) Dang, L. X.; Pettitt, B. M. *J. Am. Chem. Soc.* **1987**, *109*, 5531. (c) Pettitt, B. M.; Rossky, P. J. *J. Chem. Phys.* **1987**, *86*, 6560.

(6) (a) Ravishanker, G.; Mezie, M.; Beveridge, D. L. *Faraday Symp. Chem. Soc.* **1982**, *17*, 79. (b) Tobias, D. T.; Brooks, C. L., III *Chem. Phys. Lett.* **1987**, *142*, 472. (c) Pangali, C. S.; Rao, M.; Berne, B. J. *J. Chem. Phys.* **1979**, *63*, 2334. (d) Pratt, L. R.; Chandler, D. *J. Chem. Phys.* **1977**, *67*, 3683.

(7) Jorgensen, W. L. *J. Am. Chem. Soc.* **1989**, *111*, 3770.

0002-7863/90/1512-5716$02.50/0